Nanometric muon beam emittance from e^+ annihilation on multiple thin targets

O. R. Blanco-García[*] and A. Ciarma

INFN-LNF, Via E. Fermi 40, 00044 Frascati, Rome, Italy

The production of a low emittance muon beam is interesting for muon collider projects. In such context we study the production of positive and negative muon beams at 22 GeV, from e^+ beam-vs-fixed target collisions, with a very small transverse and longitudinal emittance of 25 π nm rad and 3×1 π mm GeV, respectively. In order to cope with the small conversion efficiency of positrons into muon pairs and the divergence of the beams, we connect thin targets by a quadrupole-only transport line common to three beams (μ^+, μ^-, and e^+) at two different energies (μ at 22 GeV and e^+ at 44 GeV), where the line is specially designed to match the muon beam phase space over $\pm 5\%$ energy spread and to mitigate the effect of multiple scattering with the targets on all beams. The transport line allows us to use a larger fraction of target material, increasing the muon population by a factor of 10 per positron bunch and splitting the power deposition over 20 to 40 targets, while keeping the muon beam emittance equal or similar to one from a single thin target of 1% of a radiation length. It might be possible to integrate this line into an accumulator ring in order to increase the muon bunch population over hundreds of positron bunches.

I. INTRODUCTION

Muon colliders have recently gain popularity in the high energy accelerator research community because of their potential to produce lepton collisions, i.e., collision of pointlike particles, at very high energy with smaller accelerator circumferences when compared to other lepton colliders limited by synchrotron radiation [1]. However, these types of colliders are still required to demonstrate their feasibility due to challenging technological requirements to produce an intense bunch population with a small emittance and high energy reach, suitable for the exploration of particle physics in a new domain.

The muon accelerator program (MAP) [2] has already advanced the initial studies for a possible muon collider reaching high luminosity in the TeV scale where positive and negative muon beams are produced as tertiary particles, from proton vs target collisions, with a very large transverse (4D) and longitudinal (+2D) emittance that is cooled down in later stages. Progress has been achieved in a small scale 4D emittance cooling test by the Muon Ionization Cooling Experiment (MICE) group [3], while, 6D-cooling remains yet untested.

Alternatively, it is possible to produce muon beams as secondaries from e^+e^- annihilation. The LEMMA (Low EMittance Muon Accelerator) project [4–7] is studying the possibility to produce one intense bunch with an extremely small normalized emittance of the order of $\epsilon_n = 0.04$ π μm rad from the accumulation, in two small accumulator rings, of a hundred to a thousand low charge muon bunches produced from e^+e^- annihilation of a low emittance positron beam impinging on a thin fixed target, see Fig. 1.

A target is considered thin if the thickness of the material traversed by the positron beam, interacting to produce muons, is only a few percent of radiation length X_0 irrespective of the transverse dimensions. In the case of the initial LEMMA concept, the target material is Beryllium (Be) and the target thickness is 3 mm, equivalent to $0.88\% X_0$.

The LEMMA parameters are challenging because the low muon production efficiency from positrons forces the beams to pass multiple times over a single thin target, which leads to unavoidable emittance growth from multiple scattering [8] and also large energy deposition in the target [9]. A thicker target could be considered to reduce the number of passages, but, it leads to emittance growth due to the beams divergence inside it.

In order to increase the muon production efficiency while preserving the emittance, mitigating multiple scattering and distributing the power deposition, we have created a transport line that connects multiple thin targets with a positron beam and effectively reduces the power per target
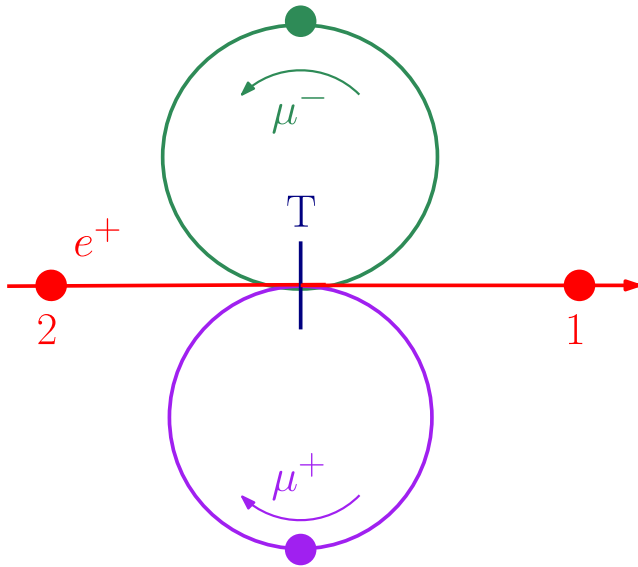
[*]oblancog@lnf.infn.it

FIG. 1. Schematic representation of the LEMMA accumulation scheme. Two muon bunches, one positive and one negative, have been produced by the interaction of the first positron bunch (1) with the target (T). Muons are recirculated in synchronicity with the arrival of a second positron bunch (2) to increase the muon bunch population with minimal emittance growth.

by at least one order of magnitude, avoids muon emittance growth and increases the bunch population by one order of magnitude, see Fig. 2. The price to pay is a longer production length, and a small deterioration of the outgoing positron bunch emittance and population per passage.

It might be possible to replace the single target in Fig. 1 by several target–line–target sequences like the one in Fig. 2, however, it will be part of further work. We concentrate in this article on the muon population and emittance produced by one positron bunch traversing multiple targets along the transport line of Fig. 2 because it gives relevant advantages with respect to a single target.

At the end of the transport line we obtain a muon bunch population on the order of 10^5 to 10^6 particles, transverse geometrical emittance of 20 to 25 π nm rad, and longitudinal emittance of 3×1 π mm GeV varying depending on the target material, and the positron beam energy. This emittance is still a factor of 100 larger in transverse and a factor of 10 larger in longitudinal compared to what was initially projected by LEMMA, however, it is the smallest emittance and largest muon population achieved with 2 T quadrupole magnets at a gradient of 525 T/m, inspired by the CLIC QD0 prototype [10].
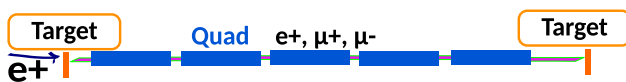

FIG. 2. Schematic diagram of the transport line. Three beams are focused at each target (μ^+, μ^-, and e^+) to mitigate multiple-scattering while chromaticity is cancelled for the muon beams.

In the following section we review few parameters that are relevant for the studies shown. In Sec. III we introduce the optics design of the transport line. Section IV is dedicated to results of muon production from beams at different energies and target materials, making emphasis in the positron and muon phase spaces. In Secs. V and VI we conclude on the parameters of the transport line, and comment on its inclusion into a ring designed for large energy acceptance.

II. MUON EMITTANCE AND PRODUCTION EFFICIENCY

The muon transverse geometrical emittance, ϵ_μ, for a thin target is

$$\epsilon_\mu = \sigma_{e^+} \cdot \sigma'_\mu(E_{e^+}), \tag{1}$$

i.e., the product of the positron beam size σ_{e^+} when crossing the target and the divergence of the produced muon beam σ'_μ from the kinematics of the target collision with a positron beam at some energy E_{e^+}. One could approximate the divergence to be 0.1 to 0.5 mrad for a positron beam at 43.72 to 45 GeV, respectively. See Table I where we list the main parameters of the muon production obtained from simulations with MUFASA [11], benchmarked with GEANT4 [12].

The muon longitudinal emittance, in the same manner, comes from the product of the positron bunch length and the energy spread produced by the kinematics of the collision. We assume here the previously studied parameters of a 6 or 27 km long positron ring in Refs. [13,14] with a bunch length of 3 mm and remark that there is no phenomena perturbing the bunch length, so it is fixed by the incoming positron beam. With respect to the muon beam energy, the amount of synchrotron radiation in the transport line is negligible while the energy loss from interacting with the target is small for a thin target and only becomes significant when passing several radiation lengths of material. The energy spread of the outgoing muon beam ranges from 1 to 10% of half the positron beam energy in the range of 43.72 to 45 GeV, respectively (See Table I). Therefore, the longitudinal emittance is in the order of 6.8 π mm GeV ($3 \times 0.10 \times 45/2$ π mm GeV) and could be as low as 0.7 π mm GeV ($3 \times 0.01 \times 43.72/2$ π mm GeV).

The muon pair production efficiency eff has been defined in [4] as the ratio of muon pairs ($\mu^\pm$, or simply μ) per positron impinging on a fixed target. LEMMA estimated that $eff = 7 \times 10^{-8} \mu/e^+$ from a 3 mm long Beryllium (Be) target and $E_{e^+} = 45$ GeV. See Table I.

III. OPTICS OF THE TRANSPORT LINE

The transport line is conceived to transport three particles types (μ^+, μ^-, and e^+) at two different energies (μ at about 22 GeV and e^+ at twice the energy), see Fig. 2.

TABLE I.   Muon production efficiency eff, divergence σ'_μ and energy spread δE_μ as a function of the positron beam energy E_{e^+}. The muon energy and divergence have a flat distribution. Efficiency has been estimated for 1% of a radiation length of Beryllium (3.5 mm of material). The muon beam divergence and energy spread are given by the collision kinematics.

E_{e^+} (GeV)	eff $(10^{-8}\mu/e^+)$	σ'_μ (mrad$_{rms}$)	(mrad$_{max}$)	E_μ (GeV)	δE_μ (%$_{rms}$)	(%$_{max}$)	$E_\mu(1\pm\delta E_\mu)$ Min/Max (GeV)
43.72	2.3	0.07	0.16	21.860	1.40	2.9	21.20/22.50
43.80	3.0	0.14	0.26	21.900	2.86	4.9	20.82/22.98
44.00	4.6	0.23	0.42	22.000	4.81	8.3	20.17/23.83
44.50	7.1	0.37	0.67	22.250	7.85	13.6	19.44/25.56
45.00	8.7	0.47	0.83	22.500	9.90	17.0	18.67/26.33
46.00	10.9	0.62	1.11	23.000	12.91	22.6	17.80/28.19

Several contributions to emittance growth act together to deteriorate the quality of a beam. In particular, we are concerned with the multiple scattering of muons and positrons inside the target that contributes to the growth of the beams divergence, and also with the chromaticity introduced by quadrupoles in the line because of the large energy spread of the muon beam and the positron energy loss associated with bremsstrahlung.

The effect of multiple scattering on the positron beam was studied in [13] where we concluded that a $\beta^*_{e^+} = 50$ cm was enough to produce a beam divergence larger than the contribution from multiple scattering in approx. $1\%X_0$ of Beryllium over a hundred turns (3.5 mm of Be material is equivalent to $1\%X_0$). We note that the transverse emittance of the positron beam used in those studies was $6\,\pi$ nm rad.

The case of muon multiple scattering is more significative because its contribution to divergence grows inversely proportional to energy, $1/E$ [4]; the muon beam has only half of the positron beam energy and it passes a thousand times through target material. A recent publication explored values of β^*_μ in the range of 100 to 10 cm for a monochromatic beam to evaluate this situation [15], however, proved not enough as a $\beta^*_\mu < 1$ cm is required to mitigate the effect over one to two thousands turns, equivalent to crossing more than 10 to 20 radiation lengths of material. We have theoretically explored more intense focusing and concluded that such a small β^*_μ requires an extremely high gradient on the order of 20 kT/m and therefore is beyond the scope for the moment. We therefore design our transport line with a gradient close to 500 T/m, which has been studied for the CLIC QD0 project and tested in a prototype [16].

The chromaticity introduced by the transport line at two different energies has also been addressed. For the muon beam we have designed a first order apochromatic lattice [17] with a $\beta^*_\mu = 20$ cm over $\pm5\%$ energy spread. We have modified the initial concept of Lindstrøm and Adli to produce the $\beta^*_{e^+} = 50$ cm at twice the muon beam energy (the positron beam energy). For the positron beam chromaticity is not cancelled. In order to reduce the impact on

the positron beam emittance we have used the Simplex minimization algorithm in MAD-X [18] with constraints on the twiss and chromatic functions for several energy offsets around the muon and positron beam energies while varying the length and strength of the quadrupoles and also the length of few drift spaces.

Table II shows the main parameters of the design done in MAD-X, while Table III shows the detailed quadrupole

TABLE II.   Transport line parameter table.

Parameter	Unit	Value
L*	cm	10
β^*_μ	cm	20
$\beta^*_{e^+}$	cm	50
Total length	m	13.455
Maximum grad	T/m	525
Minimum drift	cm	10
Magnet aperture radius	mm	4

TABLE III.   Quadrupoles Q1 to Q6 k_1 component, equivalent gradient for a 22.5 GeV muon beam, length and drifts D1 to D6. This list corresponds to half of the lattice, the second half is an antisymmetric reflection, drifts are equal and magnet polarity is reversed.

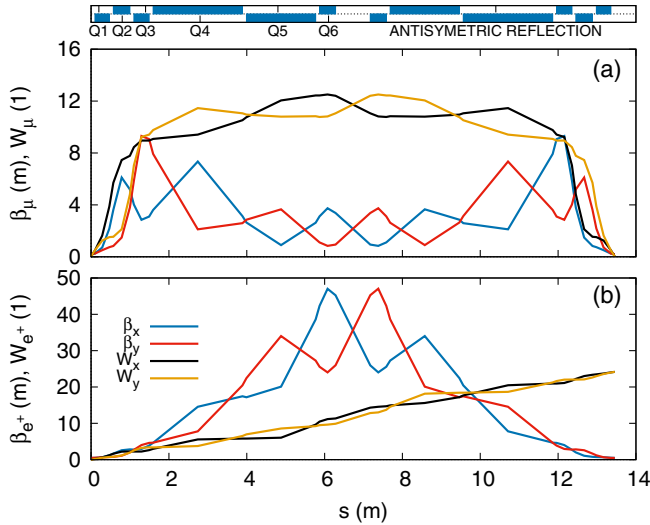| Name	k_1 (m^{-2})	Gradient (T/m)	Length (m)
L*			0.100
Q1	−7	−525.3	0.371
D1			0.101
Q2	7	525.3	0.426
D2			0.101
Q3	−5.759	−432.3	0.394
D3			0.101
Q4	0.543	40.8	2.297
D4			0.101
Q5	−0.761	−57.1	1.778
D5			0.101
Q6	3.388	254.2	0.410
D6			0.446

FIG. 3. (a) Twiss β_x, β_y and chromatic W_x, W_y functions along the transport line at the nominal energy for the muon beam and (b) twice the nominal energy for the positron beam. Top: we show the quadrupoles Q1 to Q6 location and the antisymmetric reflection of the quadrupole configuration to achieve the apochromaticity at the muon energy, $W_{x,y} = 0$ at $s = 0$ and $s = 13.455$ m, where the targets are located.

length, gradient and drifts for a muon beam at 22.5 GeV. Figure 3 shows the twiss β functions along the line and the chromatic functions W_x and W_y. Figure 4 shows the variation of β_μ^* and α_μ^* over $\pm 5\%$ of energy offset.

We remark that the transport line behaves the same irrespective of the beam electric charge as a result of the antisymmetry of the design.
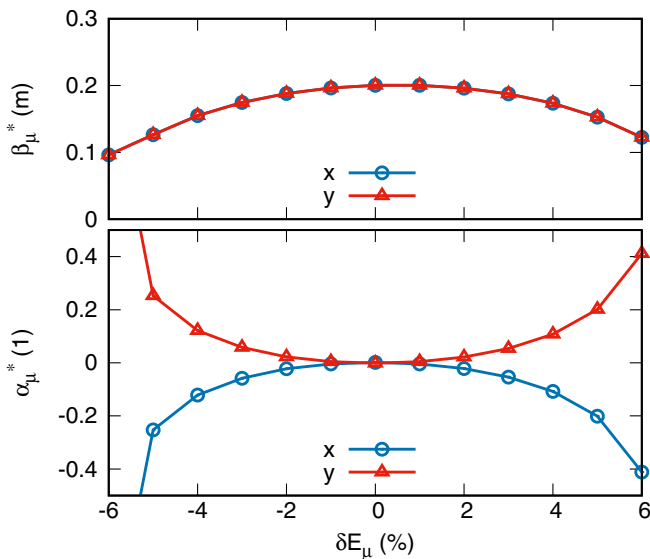

FIG. 4. Twiss parameters β_μ^* and α_μ^* for different energies ranging $\pm 6\%$ of the nominal energy.

IV. MUON PRODUCTION AND BEAM PARAMETERS

In the previous section we showed the optics parameters achieved to transport the three beams. We now show the results of muon production and tracking of the particles through the lattice.

A. Beam parameters

First, we calculate the muon beam size and emittance that matches the optics, and then will use those parameters to fix the requirements on the positron beam.

Given an energy acceptance of at least $\pm 5\%$ the muon energy and the results listed in the Table I, we can expect a beam divergence close to 0.3 mrad and energy spread close to $\pm 5\%$ from the kinematics of collision with a beam at $E_{e^+} = 43.8$ GeV. The muon beam size at the target that matches the optics can be calculated as,

$$\sigma_\mu = \beta_\mu^* \sigma_\mu' = 0.2 \text{ m} \cdot 0.3 \text{ mrad} = 60 \ \mu\text{m}. \quad (2)$$

Now, we can calculate the geometrical transverse emittance of the produced muon beam as

$$\epsilon_\mu = \sigma_\mu \sigma_\mu' = 60 \ \mu\text{m} \cdot 0.3 \text{ mrad} = 18 \ \pi \text{ nmrad}. \quad (3)$$

We assume that the positron beam at $E_{e^+} = 43.8$ GeV, has the same beam size given by Eq. (1), $\sigma_{e^+} = 60 \ \mu$m. This value is above the minimum used in [19] for simulations of power deposition in the target by a positron bunch population of 3×10^{11} particles.

As a free parameter to match the optics $\beta_{e^+}^*$ we have the positron beam emittance. Thus,

$$\epsilon_{e^+} = \frac{\sigma_{e^+}^2}{\beta_{e^+}^*} = \frac{(60 \ \mu\text{m})^2}{0.5 \text{ m}} = 7.2 \ \pi \text{ nmrad}, \quad (4)$$

which is similar to the 6πnm rad studied for the positron ring in [6].

Finally, in Table IV, we summarize the list of beam parameters obtained in this section where also include the positron ring energy spread given in [6].

B. Tracking results

We show the result of simulations done varying the positron beam energy and the target material connected by

TABLE IV. Positron and muon beam parameters matching the transport line.

Particle	Energy (GeV)	ϵ (π nm rad)	σ (μm)	σ' (mrad)	δE (%)	Type
e^+	43.8	7	60	0.12	± 0.1	(Gaus)
μ	21.9	18	60	0.30	± 5	(Flat)

the transport line. For an easier comparison we have used targets length of $1\%X_0$, which is equivalent to 3.5 mm for Beryllium.

In order to accelerate the calculation time, a dedicated fast Monte Carlo called MUFASA, written in CERN-ROOT [20], has been benched-marked with GEANT4 and MDISIM [21], and has proved to be very useful and flexible to simulate the positron-target interaction for different energies and materials, and as an interface to get tracking results. The simulation starts by generating a positron beam population that interacts with the material of the first target. Then, the outgoing positrons and produced muons are tracked through the lattice using MAD-X PTC and the output distribution is saved to calculate positron and muon beam populations, emittances, beams divergence and beam size. We repeat the previous process over many targets until the muon population does not increase significantly.

Figure 5 shows the effect of the transport line on the emittance. We compare the case of using a block of material we slice in the simulation to get the particle distribution at each step, and the case when those slices are connected by the transport line. The emittance grows inside the block due to the large divergence of the muon beam, while it stays almost constant when the target slices are connected by the transport line. In total we achieved to cross at least $0.5X_0$ of material with a small initial emittance growth.

The small change in emittance is below 30% and it is produced by higher order terms in the chromatic functions not corrected by the first order apochromat, leaving a small variation of the twiss functions as shown in Fig. 4. We can also note that the result on the vertical and the horizontal planes is similar, as expected from the antisymmetric reflection in the apochromatic design.
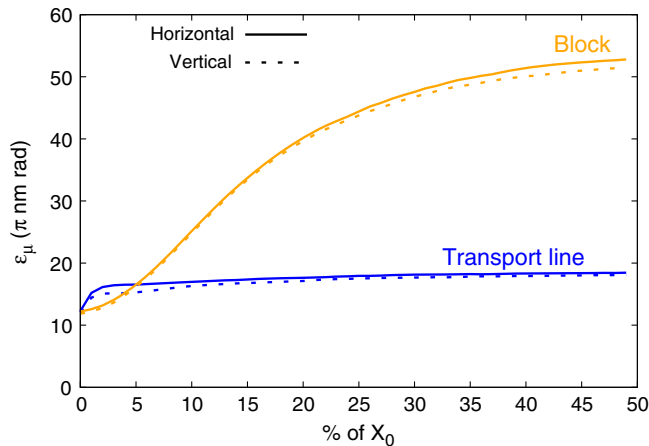

FIG. 5. Muon beam emittance when the target is sliced in units of 1% of a radiation length (X_0) of Beryllium, i.e., 3.5 mm per target. The yellow line shows the effect of the beam divergence inside the material when the targets are one after other, while the blue line shows the effect when the targets are connected by a transfer line.

Figure 6 shows the muon population growth over 50 targets. We have varied the energy of the incoming positron beam in order to see the effect on the final population and beam emittance when the muon beam energy spread surpasses the energy acceptance of $\pm 5\%$ shown in previous sections.

At the positron beam energy of 43.8 GeV, we see in Fig. 6 a matched line that preserves the muon emittance below 20 π nm rad and increases efficiency to 20×10^{-8} μ/e^+ [i.e., $10^5 \mu/(5 \times 10^{11} e^+)$], which is one order of magnitude above the case of a single target.

The muon population growth saturates at around 20 targets. This is because a big fraction of the positron population looses energy by bremsstrahlung with the target, and goes below the muon production threshold energy at $E_{e^+} = 43.7$ GeV, see Fig. 7. Increasing the positron beam energy to 44.0 GeV further increases the efficiency to 50×10^{-8} μ/e^+ [i.e., 2.5×10^5 $\mu/(5 \times 10^{11} e^+)$] because the positron population remains above the energy threshold for a longer number of targets. An emittance growth occurs over the first 5 targets due to the production of muons over an energy spread beyond the $\pm 5\%$ shown in the optics studies. The final emittance is close to 25 π nm rad.

Furthermore, an increase on the positron beam energy up to 46 GeV will also slowly increase the muon population since the transport line is unable to cope with the large muon energy spread and divergence; the muon emittance grows to 70 π nm rad.

One possible way to increase the muon production efficiency is to consider other types of materials. The transverse and longitudinal emittance shown previously depend on the fraction of a radiation length of material interacting with the positron beam, therefore, using the same $1\%X_0$ units for other materials, we can have the same beam dynamics while changing only the muon production efficiency. Table V shows a very small list of possible targets with different lengths and efficiencies that have been foreseen, while, Fig. 8 shows the muon population obtained from a 44 GeV positron beam. In particular, we highlight the possibility to use $1\%X_0$ of liquid Hydrogen (H_2) which will increase the muon population by a factor 2 with respect to Be. The target dimensions fit the 20 cm $(2L^*)$ available space among quadrupoles close to the interaction point. A possible small mismatch of the optics due to the target length seems negligible because the beta function grows just to 25 cm at the entry point of the first quadrupole magnet.

Despite of the advantages of liquid hydrogen regarding the muon production efficiency, there are materials that could become more practical solutions as they withstand better the power deposition or have dimensions that better suit the short space for beam–target interaction. Therefore, in Table V we include also carbon, a carbon based composite C/C A412 [22], liquid lithium (LLi), and a mix of 10% liquid lithium, and 90% diamond powder
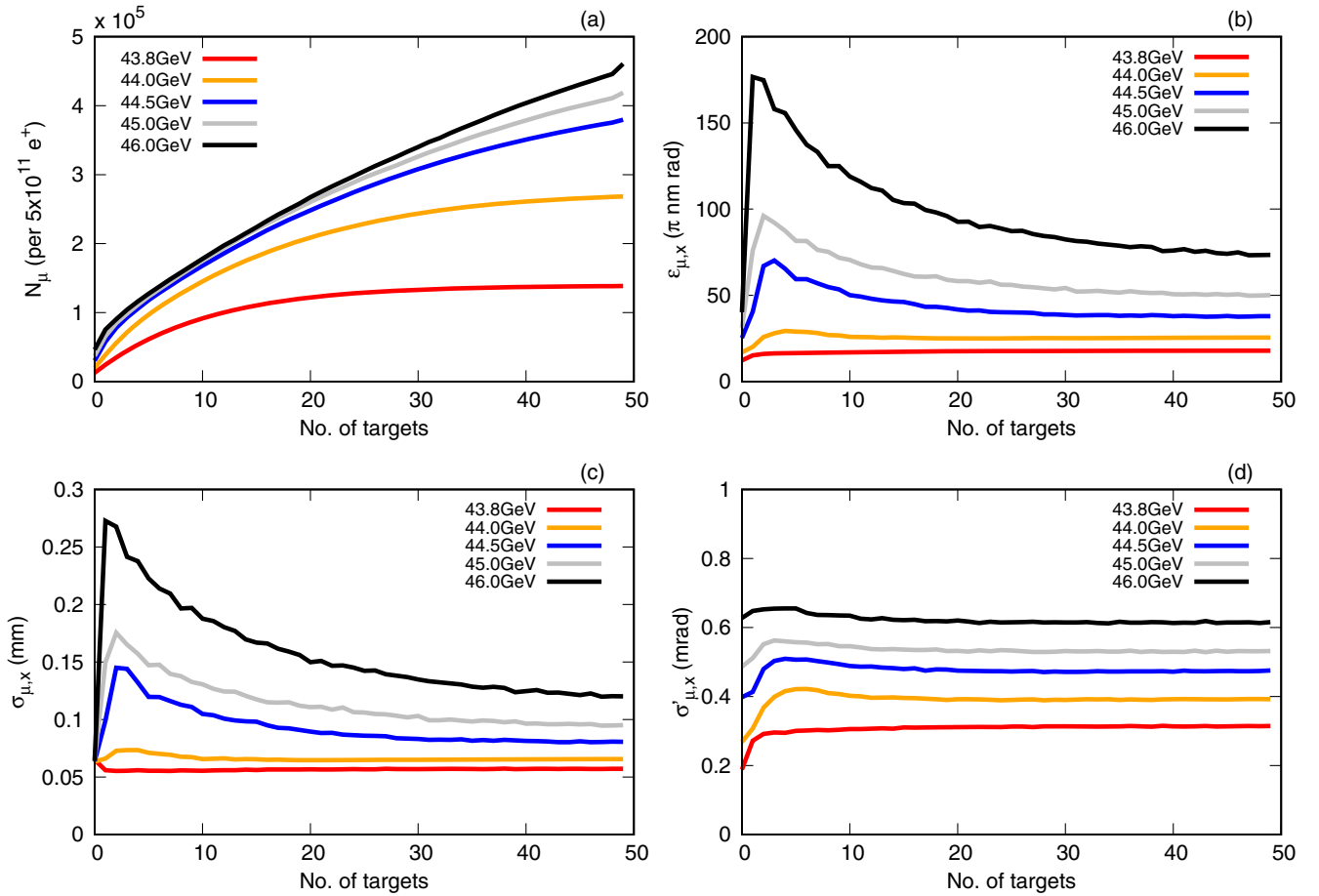
FIG. 6.   (a) Muon bunch population N_μ, (b) horizontal emittance $\epsilon_{\mu,x}$, (c) beam size $\sigma_{\mu,x}$ and (d) divergence $\sigma'_{\mu,x}$ from the simulation of a 5×10^{11} e$^+$ bunch impinging on 50 targets of $1\%X_0$ each (equivalent to 3.5 mm of Beryllium material) for five different positron beam energies. The transport line k_1 coefficients have been kept constant while changing the positron beam energy, therefore, the lattice is always matched but the equivalent gradients change slightly.
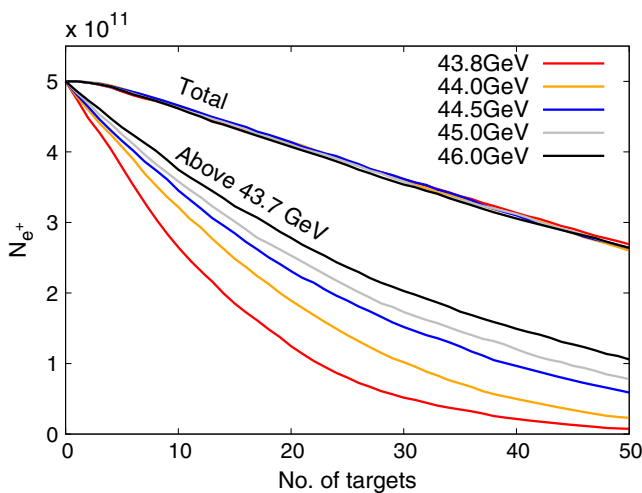

FIG. 7.   Positron bunch population N_{e^+} versus number of targets, $1\%X_0$ of Be each, for five different beam energies, counting only those above the muon production energy threshold at 43.7 GeV and the total population.

(LLi-D) [15]. The emittance obtained with these materials is equal to the case of beryllium when using the same amount of radiation lengths of material.

The reduction of the positron beam population seen in Fig. 7 is explained by the chromaticity of the transport line, unable to focus back particles that have lost partially their

TABLE V.   Muon production efficiency from a positron beam at 45 GeV interacting with beryllium, liquid hydrogen (LH2), liquid lithium (LLi), a composition of 10% liquid lithium and 90% diamond powder (LLi-D), carbon, and a carbon composite (C/C A412). Density and length for $1\%X_0$ are included.

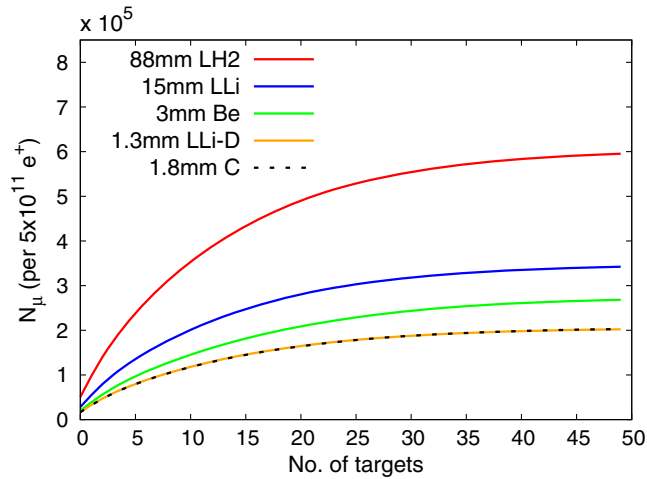| Material	Density (g cm^{-3})	$1\%X_0$ Length (mm)	eff (10^{-8} μ/e^+)
LH2	0.071	88.8	18.9
LLi	0.534	15.5	10.9
Be	1.848	3.5	8.7
LLi-D	3.221	1.3	6.3
C	2.267	1.8	6.2
C/C A412	1.7	2.5	6.2

FIG. 8.   Muon beam population N_μ vs number of targets, $1\%X_0$ each, for several materials: liquid hydrogen (LH2), liquid lithium (LLi), beryllium (Be), a combination of 10% liquid lithium and 90% diamond powder (LLi-D), and carbon (C). The positron beam population and energy are 5×10^{11} and 44 GeV, respectively.

energy due to bremsstrahlung in the target. The remaining particles in the bunch experience emittance degradation from a combination of multiple scattering in the target, and again, the increased energy spread plus the transport line chromaticity. Figure 9 shows the degradation of the positron beam emittance from 7 to 40 π nm rad over 50 targets.

V. DISCUSSION

We have shown the possibility to increase the muon production efficiency from $0.03 \times 10^{-6}\ \mu/e^+$ up to $0.2 \times 10^{-6}\ \mu/e^+$ and maintain the geometrical transverse emittance to 20 π nm rad by distributing the interaction of a positron beam over 20 beryllium targets, $0.01X_0$ each (equivalent to 3.5 mm). The longitudinal emittance is determined by the energy and bunch length of the incoming positron beam and it is preserved along the line, regardless of the target material. Any contribution to path length is much smaller than the current positron bunch length of 3 mm.

Both transverse and longitudinal emittance are larger than initially projected by LEMMA, however, this might be circumvented by reducing the incoming positron bunch length below the mm range, and studying stronger focusing gradients above 500 T/m. Alternatively, one could pursue to increase the muon population using multiple production lines.

Efficiency could be further increased to $0.5 \times 10^{-6}\ \mu/e^+$ having in mind an increase of the transverse emittance to 25 π nm rad, and the usage of 40 targets.

A factor two in efficiency could be obtained if Beryllium is replaced by more exotic materials like H_2. One percent of radiation length of H_2 corresponds to approximately 8.9 cm
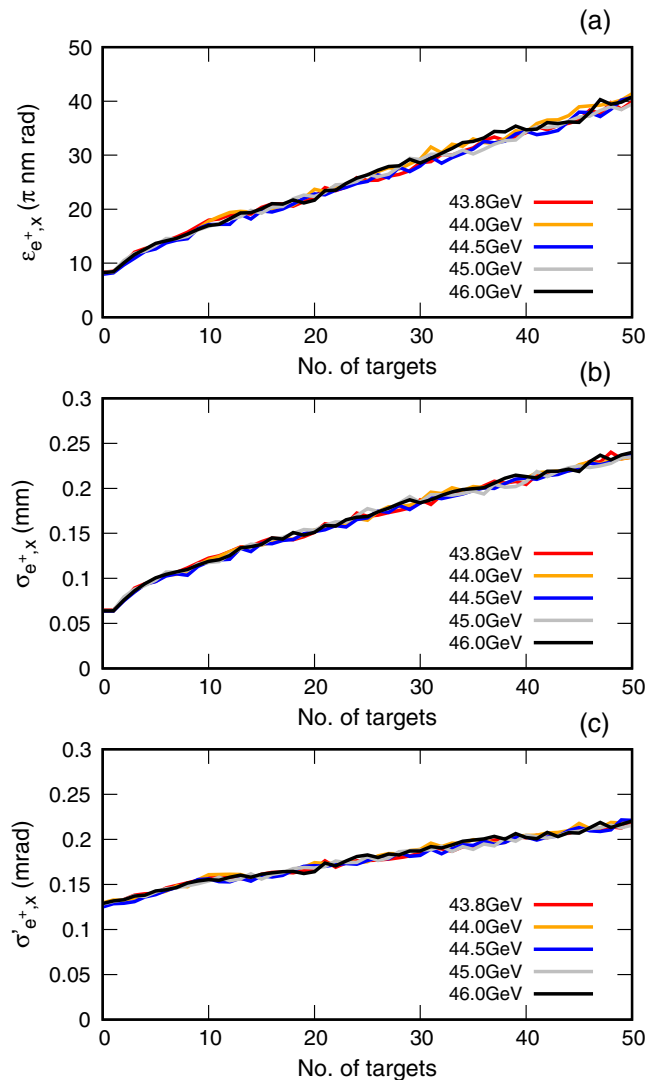

FIG. 9.   Positron bunch degradation versus number of targets, $1\%X_0$ of Be each, for five different beam energies: (a) Horizontal emittance $\epsilon_{e^+,x}$, (b) beam size $\sigma_{e^+,x}$ and (c) divergence $\sigma'_{e^+,x}$.

of material and therefore could be accommodated in the interaction region with a little tolerable mismatch due to the hourglass effect along the target.

The efficiency would also benefit from a larger energy acceptance than $\pm5\%$. It may be possible to create a second order apochromatic design with $\pm10\%$ energy acceptance, as in [17], and focalized muon and positron beams. The biggest problem is keeping the length of the transport line as short as possible to mitigate the emittance growth from chromaticity at the positron energy; however, a different approach was followed in [23] to have much shorter transport length and larger energy acceptance with no chromatic correction.

In spite of the small energy acceptance, the transport line could be included into the insertion region of an accumulator ring, in order to accumulate muons over several

positron bunches as in the LEMMA scheme. The length of the entire transport line will significantly increase the path in the accumulator and therefore reduce the number of passages possible before the beam decays. A balance between both approaches could be studied.

Furthermore, one significant drawback at the moment is the length of the production line. Having 20 targets will require 19 transport lines that will occupy 256 m. Forty targets will require 39 transport lines that will occupy about 525 m. Such a long distance of transport might raise other types of challenges related to tolerances resulting from the high gradient of the quads.

The choice of 1% allows for easier comparison of the results. However, it may seen useful to discard the possibility to use H_2 and instead put targets with larger percentage of radiation length per interaction point, allowing to reduce the length of the transport line.

Other materials could be even more interesting due to thermomechanical properties, shorter radiation lengths or availability. We have made a short list of possible materials that could be considered in further studies.

VI. CONCLUSIONS

We have shown in simulations the production of a low transverse and longitudinal emittance muon beam from positrons impinging on multiple targets in order to raise the muon population by at least one order of magnitude.

In particular, a muon beam with a population of 10^5 particles, transverse emittance of 20 π nm rad at 21.9 GeV, and longitudinal emittance of 3 π mm GeV has been obtained in simulations from a positron bunch population of 5×10^{11} particles at 43.8 GeV, focused to a beam size of 60 μm and bunch length of 3 mm, interacting with twenty Beryllium targets of 1% of a radiation length each, where the targets are connected by a transport line 256 m long.

The transport line allows to use up to 0.2 radiation lengths of material, increasing the muon population by a factor 10 in only one passage while preserving the emittance of a single thin target.

The muon beam population can be raised to 2.5×10^5 particles, i.e., a production efficiency of 0.5×10^{-6} muon pairs per e^+ by: increasing the number of targets to 40, increasing the transport line length to 525 m, and the positron beam energy to 44.0 GeV. The transverse emittance grows to 25 π nm rad due to the limits of the apochromatic correction in the transport line only valid over $\pm 5\%$ energy spread.

For a positron beam energy above 44.0 GeV, the muon population continues to increase but less efficiently as a consequence of the spread of the muon beam which is much larger than the acceptance of the transport line.

Finally, efficiency can be raised a factor two using 1% of a radiation length of liquid hydrogen, equivalent to 8.9 cm in length, with some small contribution to emittance growth

due to the mismatch of the optics parameter $\beta_\mu^* = 20$ cm at the interaction point.

Although liquid hydrogen is convenient in terms of muon production efficiency, there are power and target length considerations that can also suggest other materials, therefore, we have included a small list of possible targets that could be further studied.

As a consequence of the insertion of a transport line between targets, the total deposited power on the target by the positron and muon beams is distributed over the total number of targets, effectively reducing by one order of magnitude the power per target.

Further efforts to improve the muon production efficiency could be directed to pursue a design with larger energy acceptance at the muon beam energy, e.g., a second order apochromat transport line over $\pm 10\%$ energy spread, while minimizing the degradation of the positron beam and length of the transport line.

[1] J. P. Delahaye *et al.*, "Muon Colliders", Input to the European Particle Physics Strategy Update, January 18, 2019. arXiv:1901.06150v1.

[2] R. B. Palmer, Muon colliders, Rev. Accel. Sci. Techol. **07,** 137 (2014).

[3] MICE Collaboration, Demonstration of cooling by the Muon Ionization Cooling Experiment, Nature (London) **578**, 53 (2020).

[4] M. Antonelli, M. Boscolo, R. Di Nardo, and P. Raimondi, Novel proposal for a low emittance muon beam using positron beam on target, Nucl. Instrum. Methods Phys. Res., Sect. A **807**, 101 (2016).

[5] M. Antonelli *et al.*, Very low emittance muon beam using positron beam on target, in *Proc. 7th Int. Particle Accelerator Conf. (IPAC'16), Busan, Korea* (JACoW, Geneva, Switzerland, 2016), pp. 1536–1538.

[6] M. Boscolo *et al.*, Studies of a scheme for low emittance muon beam production from positrons on target, in *Proc. 8th Int. Particle Accelerator Conf. (IPAC'17), Copenhagen, Denmark* (JACoW, Geneva, Switzerland, 2017), pp. 2486–2489.

[7] M. Biagini *et al.*, Positron driven muon source for a muon collider: Recent developments, presented at the *10th International Particle Accelerator Conf. (IPAC'19), Melbourne, Australia, May. 2019*, paper MOZZPLS2, https://accelconf.web.cern.ch/IPAC2019/papers/mozzpls2.pdf.

[8] D. Schulte, Use of electrons in the SPS for muon collider R&D, Presentation at the Low Emittance Muon Collider Workshop, Padova, Italy. July 1-3, 2018, https://indico.cern.ch/event/719240/.

[9] M. Iafrati *et al.*, Overview of the requirements on targets: Preliminary study of muon production, Presentation at the *Muon Collider Workshop, Padova, Italy. July 1-3, 2018*, https://indico.cern.ch/event/719240/.

[10] M. Modena, CLIC QD0 "short prototype" status, contribution to *LCWS11 Workshop, Granada, Spain 2011*, arXiv:1202.5952, http://cds.cern.ch/record/1427609.

[11] A. Ciarma, MUFASA: Muon fast simulation algorithm, Istituto Nazionale di Fisica Nucleare—Laboratori Nazionali di Frascati (INFN-LNF), Frascati, Italy Technical Report No. INFN-20-07/LNF, 2020.

[12] S. Agostinelli *et al.*, GEANT4: A simulation toolkit, Nucl. Instrum. Methods Phys. Res., Sect. A **506**, 250 (2003).

[13] M. Boscolo, M. Antonelli, O. R. Blanco-García, S. Guiducci, S. Liuzzo, P. Raimondi, and F. Collamati, Low emittance muon accelerator studies with production from positrons on target, Phys. Rev. Accel. Beams **21**, 061005 (2018).

[14] S. Liuzzo, Lemma e+ring, in the *Low Emittance Muon Collider Workshop, Padova, Italy. July 1-3, 2018*, https://indico.cern.ch/event/719240/.

[15] M. Boscolo, M. Antonelli, A. Ciarma, and P. Raimondi, Muon production and accumulation from positrons on target, Phys. Rev. Accel. Beams **23** (2020).

[16] M. Modena *et al.*, Design, assembly and first measurements of a short model for CLIC final focus hybrid quadrupole QD0, *Proceedings of the 3rd International Particle Accelerator Conference, New Orleans, LA, 2012* (IEEE, Piscataway, NJ, 2012). THPPD010. https://accelconf.web.cern.ch/IPAC2012/papers/thppd010.pdf.

[17] C. A. Lindstrøm and E. Adli, Design of general apochromatic drift-quadrupole beam lines, Phys. Rev. Accel. Beams **19**, 071002 (2016).

[18] MAD-X: Methodical Accelerator Design. http://madx.web.cern.ch/madx.

[19] D. Alesini *et al.*, Positron driven muon source for a muon collider, arXiv:1905.05747.

[20] CERN root, a data analysis framework. https://root.cern.ch.

[21] H. Burkhardt and M. Boscolo, Tools for Flexible Optimisation of IR Designs with Application to FCC, in *Proc. 6th Int. Particle Accelerator Conf. (IPAC'15)* (JACoW, Geneva, Switzerland, 2015), pp. 2072–2074, https://accelconf.web.cern.ch/IPAC2015/papers/tupty031.pdf.

[22] F. L. Maciariello *et al.*, High Intensity beam test of low Z materials for the upgrade of SPS-to-LHC transfer line collimators and LHC injection absorbers, in *Proceedings of IPAC2016, Busan, Korea*, TUPMB052, https://accelconf.web.cern.ch/IPAC2016/papers/tupmb052.pdf.

[23] O. R. Blanco-Garcia *et al.*, Multitarget lattice for muon production from e+beam annihilation on target, contribution to the 10th International Particle Accelerator Conf. (IPAC'19), Melbourne, Australia, May 2019, paper MOPRB003, http://jacow.org/ipac2019/papers/moprb003.pdf.